JOURNAL OF THE KOREAN ASTRONOMICAL SOCIETY
35: 105 ~ 110, 2002

VLA AMMONIA LINE OBSERVATIONS OF THE YOUNG STELLAR OBJECT IRAS 19550+3248

HO-GYU LEE[1], BON-CHUL KOO[1], YONG-SUN PARK[1], AND PAUL T. P. HO[2]
[1]Astronomy Program, SEES, Seoul National University, Seoul 151-742, Korea
E-mail: koo@astrohi.snu.ac.kr; yspark@astro.snu.ac.kr
[2]Harvard-Smithsonian Center for Astrophysics, 60 Garden Street, Cambridge, MA 02138, U. S. A.
(Received Feb. 23, 2002; Accepted Apr. 26, 2002)

ABSTRACT

We present the results of VLA NH_3 (1,1) and (2,2) line observations of the young-stellar object (YSO) IRAS 19550+3248. The integrated intensity map of the NH_3 (1,1) line shows that there are two ammonia cores in this region; core A which is associated with the YSO, and core B which is diffuse and located at the northeast of core A. Core A is compact and elongated along the east-west direction (0.07 pc×0.05 pc) roughly perpendicular to the molecular outflow axis. Core B is diffuse and extended (0.18 pc×0.07 pc). NH_3 (2,2) line is detected only toward core A, which indicates that it is hotter ($\sim$ 15 K), presumably due to the heating by the YSO. The NH_3 (1,1) line toward core A is wide ($\Delta v \gtrsim 3$ km s^{-1}) and appears to have an anomalous intensity ratio of the inner satellite hyperfine lines. The large line width may be attributed to the embedded YSO, but the hyperfine anomaly is difficult to explain. We compare the results of NH_3 observations with those of previous CS observations and find that the CS emission is detected only toward core A and is much more extended than the NH_3 emission.

Key words: ISM: clouds — ISM: individual (IRAS 19550+3248) — ISM: molecules — stars: formation

I. INTRODUCTION

IRAS 19550+3248 is a young-stellar object (YSO) deeply embedded in a molecular cloud (5). The cloud is small (4′ × 7′) and located at the tip of a long ($\sim$ 1°) filamentary molecular cloud. The molecular cloud appears to coexist with the supernova remnant (SNR) CTB 80 on the sky, but there is no evidence for the interaction between the two. The kinematic distance to the cloud is 2 kpc. Near infrared observation between 2 and 25 μm shows that the YSO is a class I object with the bolometric luminosity of 150 $L_\odot$. It appears to be one of those sources with a large ratio of the luminosity to the mass of the parental molecular cloud which could be an indication of the shock-induced star formation (14).

IRAS 19550+3248 is associated with a dense CS core, which has a very large velocity dispersion (7). The observed CS line width (2.4 km s^{-1}) is much larger than the average line width (0.5 – 1.0 km s^{-1}) of CS cores in dark clouds. The large velocity dispersion is due to small (< 0.05 pc) clumps moving supersonically in the beam. The virial mass implied from the velocity dispersion is greater than the mass derived from the total CS flux by an order of magnitude, which suggests that the clumps are dispersing. The dispersal may be due to the high-velocity outflow associated with IRAS 19550+3248.

In this paper we present the results of VLA NH_3 line observations toward IRAS 19550+3248. An advantage of the NH_3 observation is that it provides a reliable estimate of kinetic temperature of molecular material through the ratio of inversion transition lines in different metastable states. It is also interesting to compare the results with those of previous CS observations. Previous studies showed that CS has generally more extended emission than the NH_3 despite its higher critical density, which is not clearly understood.

II. OBSERVATION

We carried out NH_3 (1,1) and (2,2) line observations using the VLA of NRAO[1] in the D-configuration. Table 1 shows the VLA observing parameters. We used the 4IF mode which splitted the 256-channel correlator into four sections to allow simultaneous observations of the NH_3 (1,1) and (2,2) lines with two circular polarizations for each line. The bandwidth covers the main and inner-satellite quadrupole hyperfine components separated by $\sim$ 1 MHz for the NH_3 (1,1) transition. To calibrate the variations of the gain and phase of array, we observed 2021+317 at every 17 minutes. The flux calibrator was 3C 286 which was assumed to have a flux density of 2.44 Jy, and the bootstrapped flux of 2021+317 was 1.72 ± 0.02 Jy. The data were edited and calibrated within Astronomical Image Processing System (AIPS) software provided by the NRAO.

We made and cleaned maps with the AIPS task MX. We used natural weighting and Hanning smoothing to

Corresponding Author: B.-C. Koo

[1]The National Radio Astronomy Observatory is operated by Associated Universities, Inc. under agreement with the National Science Foundation.

Table 1. Observing Parameters

Parameter	Value
Array	VLA-D
Date	December 19, 1993
Rest frequencies	23.694495 [NH_3 (1,1)] GHz
	23.722633 [NH_3 (2,2)] GHz
Field center	($19^h55^m00^s$, +32°48′28″)
Bandwidth	3.125 MHz
Velocity center	+13.0 km s^{-1}
Velocity resolution	1.24 km s^{-1}
Phase calibrator	2021+317
On-source time	5 hr 20 min.
Primary beam	~ 2′
Synthesized beam	3″.8 × 3″.4 (p.a. −89°)
1σ noise	2.3 mJy $beam^{-1}$

obtain a high sensitivity. The noise level (1 σ) of the final maps was 2.3 mJy $beam^{-1}$ per channel which was ~ 30 % higher than the theoretical value. We averaged the line-free channels of NH_3 (1,1) and (2,2) maps to form a continuum map. There was no continuum source brighter than 1.4 mJy (> 4 σ).

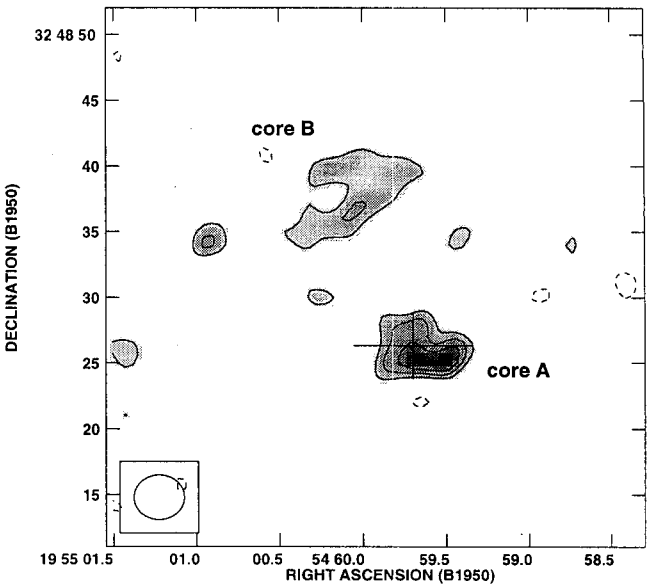

Fig. 1.— The intensity distribution of the NH_3 (1,1) emission integrated over v_{LSR} = 11.1 to 15.5 km s^{-1}. Contour levels are −17, −12, 12, 17, 22 and 27 mJy $beam^{-1}$ km s^{-1}. The cross indicates the position of the K band image of protostar at ($19^h54^m59^s.7$, +32°48′26″.3).

III. RESULTS

Figure 1 shows the intensity distribution of the NH_3 (1,1) line emission integrated over the velocity range from 11.1 to 15.5 km s^{-1}. The cross indicates the positon of IRAS 19550+3248 in K-band (6), and we use it as the postion of the YSO. Figure 1 shows that there are two cores in this region: the brighter one (core A) which coincides with the YSO, and the fainter one (core B) at its northeast. Core A is elongated (~ 7″ × 5″) along the east-west direction. There is a high-veliocity, bipolar CO outflow with blue and red peaks separated by 1′ along the north-south direction (Koo et al. 1994) and the elongation is roughly perpendicular to the outflow axis. The NH_3 emission attains a maximum at the south of the YSO. Core B is located at ~ 15″ northeast of IRAS 19550+3248. It is diffuse and extends over ~ 15″ × 7″.

Central condensations have been observed toward sevaral class 0 and I objects including IRAM 04191+1523, HH 212, L1634, HH 111, NGC 2023, HH 24-25, and HH 211 (Wiseman et al. 2000, 2001; Wootten et al. 2001). The observations show that the flattened structures traced by ammonia in these objects are generally perpendicular to the outflow axis and their velocity gradient along the disk is consistent with rotational motion. It is highly likely that the core A of IRAS 19550+3248 is also a rotating disk lying perperdicular to the outflow axis. However, the limited sensitivity does not allow further conclusive interpretations.

Figure 2 shows the NH_3 (1,1) and (2,2) spectra of the two cores. For each core, we show average spectra and the spectra toward its peak position. The average spectra were obtained by averaging the spectra with integrated intensity greater than 10 mJy $beam^{-1}$ km s^{-1} in Figure 1. Both the peak and average spectra seem to indicate that the main hyperfine component of core A may have two velocity components, which are centered at 12.1 and 14.9 km s^{-1}, respectively. The 12.1 km s^{-1} component is brighter than the 14.9 km s^{-1} component. On the other hand, core B has a single, narrow velocity component centered at 12.4 km s^{-1}. In core B, the satellite hyperfine lines are detected at expected positions with marginal (2.5σ) intensity. In core A, on the other hand, the component on the blue side is missing, while the component on the red side appears to be shifted by +1.0 km s^{-1} from the expected position. We will discuss this apparent intensity anomalies in § 4.2. NH_3 (2,2) line is detected only toward core A, which indicates that core A is hotter than core B. Table 2 summarizes the observed parameters of two cores. In Table 2, the spectral parameters, e.g., center velocity v_0, velocity width (FWHM) Δv, the maximum intensity of the (1,1) main and satellite lines $T_m(1,1)$ and $T_s(1,1)$, are obtained from least-squares fits. In the least-squares fit, we used three Gaussians representing one main and two satellite hyperfine components. The separations among the Gaussian components were fixed and the satellite lines were assumed to have equal intensities. Considering the low S/N ratio of the spectra, we assumed a single velocity component for core A too. The results of the least-squares fit are shown in Figure 2. The $T_m(2,2)/T_m(1,1)$ in Table 2 is the ratio

Table 2. Parameters of NH_3 cores

Parameter		Core A	Core B
Peak position			
$(\alpha_{1950}, \delta_{1950})$		$(19^h54^m59^s.68, 32°48'25''.5)$	$(19^h55^m00^s.32, 32°48'33''.0)$
$(v_0, \Delta v)^a$	(km s^{-1})	(12.9, 3.8)	(12.4, 1.2)
$T_m(1,1)^a$	(K)	1.4	1.8
$T_s(1,1)/T_m(1,1)^a$		0.2	0.48
$T_m(2,2)/T_m(1,1)$		0.4 ± 0.1	< 0.35
T_{rot}	(K)	$14.7^{+1.9}_{-1.3}$	< 14
$N(NH_3)^b$	(cm^{-2})	$1.1^{+0.6}_{-0.4} \times 10^{15}$	7.5×10^{14}
Whole cloud			
Angular extent		$\sim 7'' \times 5''$	$\sim 19'' \times 7''$
$(v_0, \Delta v)^a$	(km s^{-1})	(12.6, 3.3)	(12.8, 2.6)
$T_m(1,1)^a$	(K)	1.0	0.71
$T_s(1,1)/T_m(1,1)^a$		0.14	0.35
$T_m(2,2)/T_m(1,1)$		0.20 ± 0.09	< 0.28
T_{rot}	(K)	$12.8^{+0.7}_{-1.3}$	< 15
$N(NH_3)^b$	(cm^{-2})	$5.6^{+3.9}_{-2.2} \times 10^{14}$	3.8×10^{14}
$\bar{N}^b_{H_2}$	(cm^{-2})	$5.6^{+3.9}_{-2.2} \times 10^{22} X_{-8}^{-1}$	$3.8 \times 10^{22} X_{-8}^{-1}$
Mass^b	($M_\odot$)	$\sim 2.0 X_{-8}^{-1}$	$\sim 1.3 X_{-8}^{-1}$

[a] Errors are not listed for these parameters because the formal errors in least-squares fits are too small. For comparison, rms (1σ) noises in the peak and average spectra are 0.29 K and 0.14 K, respectively.
[b] For core B, we assumed that $T_{rot} = 10$ K.

at line peaks.

We have estimated the NH_3 column densities of cores A and B. The rotational temperature T_{rot} is derived first using the intensity ratio between lines in different K ladder (3)

$$T_{rot} = \frac{-41.5}{\ln\left[-\frac{0.282}{\tau(1,1;m)} \ln\left\{1 - \frac{T_B(2,2;m)}{T_B(1,1;m)}(1 - e^{-\tau(1,1;m)})\right\}\right]}, \quad (1)$$

where $\tau(i,i;m)$ and $T_B(i,i;m)$ are the peak optical depth and brightness temperature of the main component of (i,i) inversion transition, respectively. The $\tau(1,1;m)$ is found from the intensity ratio of main and satellite lines of (1,1) transition. For core A, where it is not available due to anomalous line intensity ratios, it is assumed to be 2 (for the peak position) or 1 (for the averaged one). Then the NH_3 column density of the lower level of (1,1) transition *per degeneracy*, $N_0(1,1)$, is derived using its relation to the integrated intensity of the (1,1) main line, $\int T_B(1,1;m)dv$ by assuming the same excitation temperature,

$$\begin{aligned} N_0(1,1) &\simeq \frac{8\pi}{A(1,1;m)} \left(\frac{\nu_0}{c}\right)^3 \frac{1}{(1 - e^{-h\nu_0/kT_{ex}})} \\ &\times \frac{1}{(T_{ex} - T_{BG})} \frac{\tau(1,1;m)}{(1 - e^{-\tau(1,1;m)})} \\ &\times \int T_B(1,1;m)dv, \end{aligned} \quad (2)$$

where ν_0 is the frequency of the transition and the other simbols have their usual meanings. The $A(1,1;m)(= 7.5 \times 10^{-7} s^{-1})$ is the weighted sum of hyperfine Einstein coefficients by its statistical weight contributing to the main component. Here we assumed that the population among hyperfine levels distributes in proportion to their statistical weight because energy difference is negligible.

The total column density of NH_3 is estimated using the relation,

$$\begin{aligned} N_{tot} &\simeq 18 N_0(1,1) \frac{[n(0,0) + n(1,1) + n(2,2)]}{n(1,1)} \\ &= 6 N_0(1,1) \left(e^{23.1/T_{ex}} + 3 + 5e^{-41.2/T_{ex}}\right), \end{aligned} \quad (3)$$

where the summation is restricted to the lowest levels ($J = K$) of each K ladder, since the higher levels ($J > K$) within a ladder will not be populated due to large Einstein coefficients. The results are presented in Table 2. In Table 2, $N(NH_3)$ is the total column density of NH_3, $\bar{N}(H_2)$ is the average H_2 column density obtained by assuming that $X_{NH_3} \equiv [NH_3]/[H_2] = 10^{-8} X_{-8}$ (2), and M is the mass of the cloud including the cosmic abundnace of helium.

The column densities in Table 2 are the *beam-averaged* column densities. One can also derive the column density $N_0(1,1)$ from $\tau(1,1;m)$ without relying on the observed value of the $\int T_B(1,1;m)dv$. Since

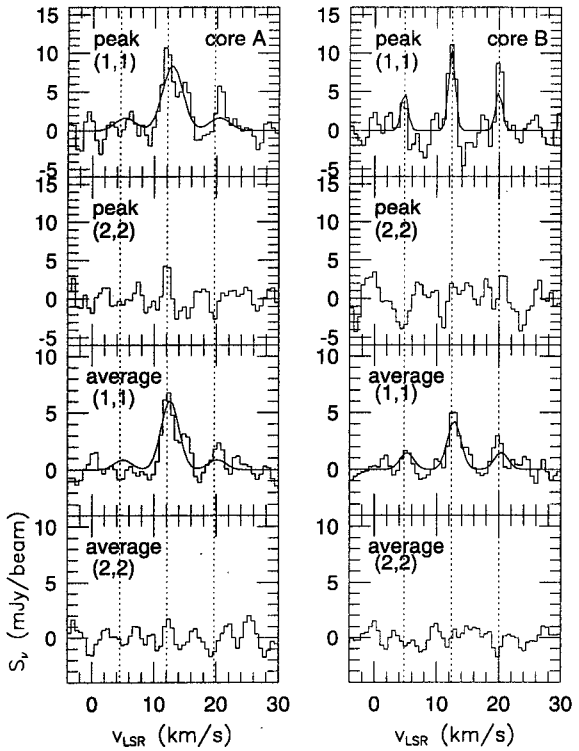

Fig. 2.— NH_3 (1,1) and (2,2) spectra toward cores A and B. Upper panels are the spectra toward the peak positions of core A ($19^h54^m59^s.683, 32°48'25''.0$) and core B ($19^h55^m0^s.317, 32°48'33''.0$). Lower panels are the average spectra of cores A and B. The dotted lines in the middle are the reference lines to mark the velocity of the peak intensity of the (1,1) lines, while the other two lines on sides mark the 'expected' positions of inner satellite hyperfine lines, i.e., the velocities shifted from the main line by ±7.6 km s^{-1}. The smooth solid profiles overlaid on the (1,1) spectra show the results of the least-sqaures fit.

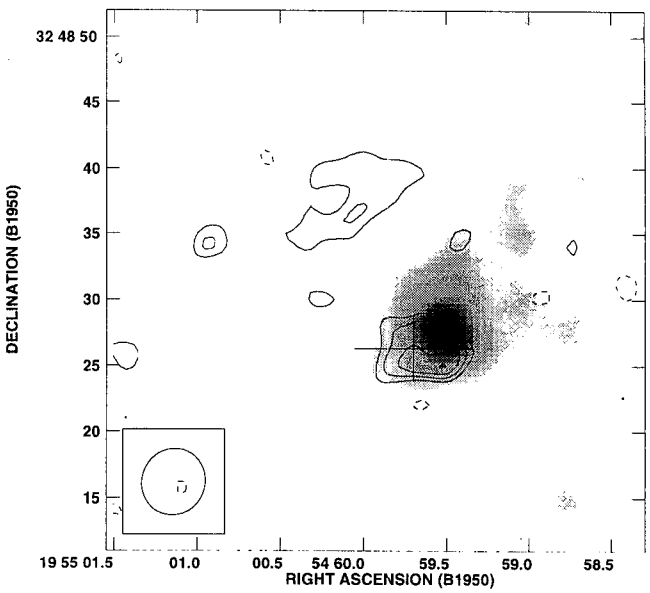

Fig. 3.— Integrated intensity contour map of NH_3 (1,1) emission overlaid on the CS J=2–1 map of Lee et al. (1997). The grey scale varies linearly from 0.1 to 1.0 Jy $beam^{-1}$ km s^{-1}. The circle in the lower left box represents the beam size of the CS observation.

it is determined by the line ratio which is not subject to the beam-filling factor, the column density calculated in this way can be compared with the above ones to estimate the beam-filling factor (13). The beam-filling factor is found to be $\sim 13 - 18\%$.

IV. DISCUSSION

(a) Comparision with CS Observation

In Figure 3 we compare the integrated intensity distribution of the NH_3 (1,1) emission with that of the CS J=2–1 emission obtained by (7). The CS data was obtained by using the Nobeyama Millimeter Array in C and D configurations, which provided a beamsize of $5''.0 \times 4''.8$ and was sensitive to structures with angular sizes of $76''$. In contrast to the NH_3 emission, the CS emission was detected only toward core A. It comprises a compact component and a diffuse envelope extended to the northwest. The total mass is 4.9 $M_\odot$ and most (~80%) of the mass resides in the compact component. The CS emission is much more extended ($\sim 15''$) than the NH_3 emission and attains a maximum at $\sim 3''$ (or 0.03 pc) north of the NH_3 peak.

Despite its higher critical density, the trend for CS to have a more extended emission than the NH_3 has been observed in previous studies (e.g., Zhou et al. 1989; Myers et al 1991; Pastor et al. 1991). Several mechanisms have been proposed to explain the peculiar spatial distribution of the two molecules. () proposed that the CS line emission could be scattered more effectively than the NH_3 (1,1) line emission in the low-density envelope because the NH_3 molecules in the (1,1) level are distributed over hyperfile levels. On the other hand, some authors attributed the peculiarity to the difference in the chemistry of two molecules. Taylor, Morata, & Williams (1996, 1998), for example, proposed a chemical model where molecular clouds are clumpy and most clumps dissipate before NH_3 abundances build up to significant level but contain substantial CS. Another possibility is the enhancement of CS abundance by shock. Model calculations on shock chemistry showed that NH_3 is hardly affected by the shock while the sulphur-bearing molecules are enhanced (Iglesias & Silk 1978; Hartquist et al. 1980; Mitchell 1984). In core A, NH_3 core appears to surround the southern part of the extended CS emission. But their line profiles are similar, e.g., both lines are wide ($\Delta v \gtrsim$ 2–3 km s^{-1}) and have double peaks at approximately the same velocities (Fig. 4). The large line width suggests that both the NH_3 and CS cores probably have been affected by the newly formed

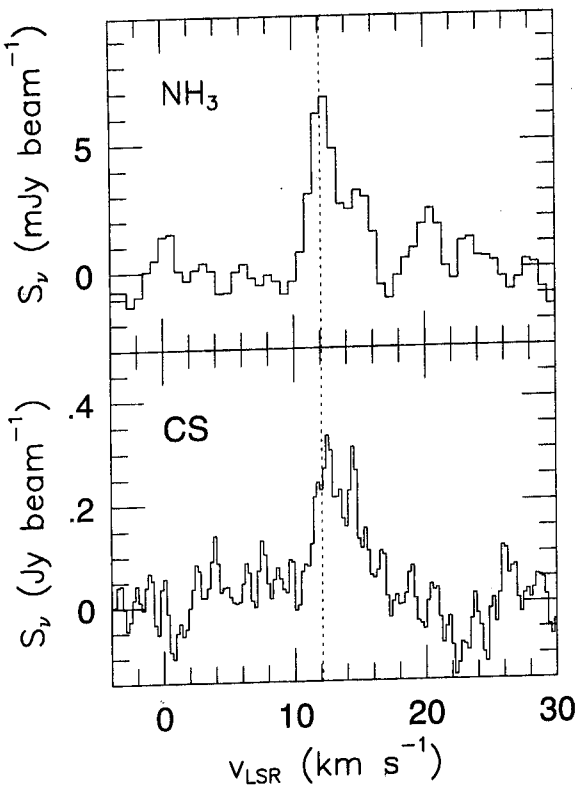

Fig. 4.— (Top) Average spectrum of NH_3 (1,1) line. (Bottom) Average spectrum of CS J=2–1 line.

stars. Therefore, a plausible explanation for the extended CS emission might be the enhancement of CS abundance by shock, perhaps driven by outflows from newly formed stars.

(b) Hyperfine Anomaly of NH_3 Line in Core A?

According to our results, the hyperfine component on the blue side, i.e., the one due to $F_1 = 1 \rightarrow 2$ transition, of the NH_3 (1,1) line appears to be missing toward core A. The component on the red side ($F_1 = 2 \rightarrow 1$) has been detected clearly at 4σ level, but its center velocity is shifted from the expected position by 1 km s^{-1}. If we naively fit a Gaussian, we obtain $T_s(1,1)/T_m(1,1)$ =0.14–0.2, which is less than the ratio (0.26) in the optically thin limit in LTE. Intensity anomalies in the inner hyperfine components of NH_3 (1,1) line have been observed previously in some sources, but they were usually weak (e.g., Stutzki et al. 1984).

Under the LTE condition, the inner satellite lines of the NH_3 (1,1) inversion line have an equal intensity, which would be between 0.26 ($\tau \ll 1$) and 1.0 ($\tau \gg 1$) times the intensity of the main line. (13) studied the non-LTE effect and concluded that it is very small for the inner satellite lines. (10) studied the possible role of systematic motion and found that, in a bundle of transitions from the (2,2) to (1,1) levels, photons emitted from one transition can be absorbed by another transition due to the systematic motion and the small frequency difference among the hyperfine transitions, resulting in drastic changes in the level populations of (1,1) sub-states. The observed trend could arise when the core expands. But none of the models could reproduce the contrast as big as what we observed in IRAS 19550+3248. It is very crucial to confirm the anomality with a better S/N ratio.

V. SUMMARY

We have made VLA NH_3 (1,1) and (2,2) line observations of IRAS 19550+3248, which is an intermediate-luminosity (150'$L_\odot$) YSO formed within a small (2 pc × 4 pc) cloud located at the tip of a long (~ 35 pc) filamentary molecular cloud. Our main results are the following:

(1) We have detected two NH_3 cores, core A and core B. Core A is compact (0.07 pc×0.05 pc) and coincides with the protostar. It is elongated along the east-west direction, roughly perpendicular to the molecular outflow axis. The mass of core A is $2.0X_{-8}^{-1}$ $M_\odot$. Core B, which is located at the northeast of core A, is faint and diffuse. Its mass is $1.3X_{-8}^{-1}$ $M_\odot$. The NH_3 (2,2) line is detected only toward core A, which might indicate the heating due to newly formed stars.

(2) While core B has a typical profile of NH_3 (1,1) spectrum, core A has an unusual spectrum: Its main hyperfine line is wide with double peaks separated by 2.8 km s^{-1}. The inner satellite hyperfine line on the red side is much stronger than the one on the blue side. The trend is consistent with the core being expanding, but the observed ratio is difficult to explain and, furthermore, the line on the red side is shifted by ~ 1 km s^{-1} from the expected velocity.

(3) We compare the NH_3 emission with previously observed CS emission. In contrast to the NH_3 emission, the CS emission was detected only toward core A. In core A, the CS emission is much more extended than the NH_3 emission. A plausible explanation for the extended CS emission might be the enhancement of CS abundance by shock, perhaps driven by outflows from newly formed stars.

This work has been supported in part by the Korea Research Foundation Grant (KRF-2000-015-DP0446).

REFERENCES

Fuller, G. A., & Myers, P. C. 1987, in Physical Processes in Interstellar Clouds, ed. G. E. Morfill & M. Scholer (Dordrecht: Reidel), 137

Hartquist, T. W., Dalgarno, A., Oppenheimer, M. 1980, Molecular diagnostics of interstellar shocks, ApJ, 236, 182

Ho, P. T. P. & Townes, C. H. 1983, Interstellar ammonia, ARAA 21, 239

Iglesias. E. R. & Silk, J. 1978, Nonequilibrium chemistry in shocked molecular clouds, ApJ, 226, 851

Koo, B.-C., Yun, M.-S., Ho, P. T. P., & Lee, Y. 1993, Interaction between the supernova remnant CTB 80 and the ambient interstellar medium: H I and CO observations, ApJ, 417, 196

Koo, B.-C., Lee, Y., Fuller, G. A., Lee, M. G., Kwon, S.-M., & Jung, J.-H. 1994, A multiwavelength study of IRAS 19550+3248: A protostar possibly formed by a cloud-cloud collision, ApJ, 429, 233

Lee, H.-G., Koo, B.-C., Park, Y.-S., & Roh, D.-G. 1997, NMA CS J=2–1 line observations of IRAS 19550+3248, PASJ, 49, 639

Mitchell, G. F. 1984, Effects of shocks on the sulfur chemistry of a dense interstellar cloud, ApJ, 287, 665

Myers, P. C., Fuller, G. A., Goodman, A. A., & Benson, P. J. 1991, Dense cores in dark clouds. VI - Shapes, ApJ, 376, 561

Park, Y.-S. 2001, Hyperfine anomalies in the ammonia (1,1) inversion transition: can they be a tracer of systematic motion?, A&A, 376, 348

Pastor, J., Estalella, R., López, R., Anglada, G., Planesas, P., & Buj, J. 1991, A CS study of star-Forming regions previously mapped in ammonia, A&A, 252, 320

Stutzki, J., Jackson, J. M., Olberg, M., Barrett, A. H., & Winnewisser, G. 1984, NH_3 hyperfine intensity anomalies, A&A, 139, 258

Stutzki, J., & Winnewisser, G. 1985, On the interpretation of hyperfine-structure intensity anomalies in the NH_3 (J, K) = (1, 1) inversion transition, A&A, 144, 13

Sugitani, K., Fukui, Y., Mizuno, A., & Ohashi, N. 1989, Star formation in bright-rimmed globules - evidence for radiation-driven implosion, ApJ, 342, L87

Taylor, S. D., Morata, O., & Williams, D. A. 1996, The distribution of CS and NH_3 in star-forming regions, A&A, 313, 269

——. 1998, The distribution of molecules in

Wiseman, J., Wootten, A., Zinnecker, H., McCaughrean, M. 2001, The flattened, rotating molecular gas core of protostellar jet HH 212, ApJ 550, 87

Wootten, A. Wiseman, J., Fuller, G. A. 2001, Gas kinematics around the youngest protostars and jets: the ammonia core encompassing IRAM04191, 199th AAS Meeting, #60.02

Zhou, S., Wu, Y., Evans II, N. J., Fuller, G. A., & Myers, P. C. 1989, A CS survey of low-mass cores and comparison with NH_3 observations, ApJ, 346, 168